Structural Engineering and Mechanics, *Vol. 67, No. 6 (2018) 565-578*
DOI: https://doi.org/10.12989/sem.2018.67.6.565

Nonlinear finite element solutions of thermoelastic flexural strength and stress values of temperature dependent graded CNT-reinforced sandwich shallow shell structure

Kulmani Mehar and Subrata K. Panda*

Department of Mechanical Engineering, National Institute of Technology Rourkela, 769008, Odisha, India

(Received June 8, 2018, Revised June 22, 2018, Accepted June 25, 2018)

Abstract. This research article reported the nonlinear finite solutions of the nonlinear flexural strength and stress behaviour of nano sandwich graded structural shell panel under the combined thermomechanical loading. The nanotube sandwich structural model is derived mathematically using the higher-order displacement polynomial including the full geometrical nonlinear strain-displacement equations via Green-Lagrange relations. The face sheets of the sandwich panel are assumed to be carbon nanotube-reinforced polymer composite with temperature dependent material properties. Additionally, the numerical model included different types of nanotube distribution patterns for the sandwich face sheets for the sake of variable strength. The required equilibrium equation of the graded carbon nanotube sandwich structural panel is derived by minimizing the total potential energy expression. The energy expression is further solved to obtain the deflection values (linear and nonlinear) via the direct iterative method in conjunction with finite element steps. A computer code is prepared (MATLAB environment) based on the current higher-order nonlinear model for the numerical analysis purpose. The stability of the numerical solution and the validity are verified by comparing the published deflection and stress values. Finally, the nonlinear model is utilized to explore the deflection and the stresses of the nanotube-reinforced (volume fraction and distribution patterns of carbon nanotube) sandwich structure (different core to face thickness ratios) for the variable type of structural parameter (thickness ratio, aspect ratio, geometrical configurations, constraints at the edges and curvature ratio) and unlike temperature loading.

Keywords: FG-CNT; HSDT; FEM; nonlinear deflection; uniform thermal environment; temperature depended properties

1. Introduction

The applications of the advanced composite material are rapidly increasing from last few decades owing to their better strength as compared to the conventional material at a specific weight ratio. Numerous efforts have been put forward by many researchers to increase the thermal, mechanical, chemical and electrical properties of the composite by introducing different kind of reinforcement materials. In 1991, an advanced reinforcement material, named as carbon nanotube (CNT) was discovered (Iijima 1991). Due to unique properties such as very high specific strength and extraordinary electrical and thermal properties with high aspect ratio (Sengupta *et al.* 2014), it attracted the attention of researcher and scientist working in this domain. The CNT is a good replacement for other available reinforcement material in hybrid composite as it not only improves the binding force between fibre and polymer, but also enhances the material properties of the hybrid composite significantly. Chen and Liu (2004) calculated the material properties of the CNT reinforced composite using the squared shape representative volume element method in combination with finite element method (FEM). Further, the Mori-Tanaka technique has been used to evaluate the effective elastic properties of the CNT reinforced composite and the elastic properties are found to be highly influenced by agglomeration and orientation of the CNT (Shi *et al.* 2004). Later, attempts have been made to evaluate the material properties of the CNT and CNT reinforced composite and it is found that the Young's modulus of the CNT varies in the range of approximately 1 TPa to 7 TPa (Li and Chou 2004, Zhang and Shen 2006, Esteva and Spansos 2009). Effect of the temperature on the material properties of CNT is frequently evaluated using molecular dynamic (MD) (Zhang and Shen 2006). Zhang *et al.* (2008) evaluated the buckling behaviour of the CNT via MD simulation. The functionally graded (FG) concept is used to obtain the effective response of the CNT reinforced composite that became a benchmark for other researchers (Shen 2009). Four different grading patterns are used namely UD (CNT is uniformly distributed throughout the curved panel), FG-X (CNT concentration is zero at the mid-plane with gradual increases toward the top and bottom surface), FG-O (CNT concentration is maximum at the mid-plane and gradually decreases toward the upper and lower surfaces) and FG-V (CNT concentration gradually increases toward the topmost surface with zero at the lowest surface). The most important advantage of the FG structure over laminated structure is the minimization of the occurrence of delamination. The effect of delamination on the deflection

*Corresponding author, Associate Professor
E-mail: call2subrat@gmail.com or pandask@nitrkl.ac.in

ISSN: 1225-4568 (Print), 1598-6217 (Online)

and stress behaviour of the laminated composite plate have studied using third-order shear deformation theory (TSDT) (Szekrenyes 2014). The natural frequency, central point deflection and stresses of the FG carbon nanotube (FG-CNT) reinforced composite plate based on the first-order shear deformation theory (FSDT) is computed (Zhu *et al.* 2012). The nonlinear bending responses of FG-CNTRC plate is investigated by means of element-free kp-Ritz method in conjunction with the FSDT and von-Karman geometrical nonlinearity (Lei *et al.* 2013). Shen and Xiang (2014) implemented higher-order shear deformation theory (HSDT) alongside the geometrical nonlinearity in von-Karman sense to examine the nonlinear frequency responses of cylindrical FG-CNTRC panel. The nonlinear central deflection values of the FG-CNTRC structure are investigated time to time by different available shear deformation theories (Kaci *et al.* 2012, Heydari *et al.* 2015) along with the computation of different structural responses of composite shell panel (Yas and Heshmati 2012, Arani and Kolahchi 2014, Szekrenyes 2014, Zhang *et al.* 2014, Kolahchi *et al.* 2014, Lei *et al.* 2014, Besseghier *et al.* 2015, Tornabene *et al.* 2016, Mehar and Panda 2016a, Mirzaei and Kiani 2016a, Madani *et al.* 2016, Bilouei *et al.* 2016, Kolahchi *et al.* 2016, Zhang 2017, Khetir *et al.* 2017, Henderson *et al.* 2018, Wang *et al.* 2018, Karami *et al.* 2018a, Karami *et al.* 2018b, Zine *et al.* 2018). Additionally, many research work has proposed to examine the structure behaviour of nanostructures.

As a design engineer, it is very important to design the composite structure with optimum strength and weight ratio. In this regard, the composite sandwich structure made by two stiff composite face-sheets at top and bottom and one soft thick core to bond both face sheets are a good option. Wang and Shen (2012a) formulated an HSDT based FG sandwich plate model reinforced with CNT to examine the nonlinear frequency and central deflection using von-Karman based geometrical nonlinearity. Further, different type shear deformation theories are implemented (Natarajan *et al.* 2014) to examine the linear frequency and central deflection of the FG-CNTRC sandwich plate with various degree of freedom at each node. The flutter behaviour of the CNT reinforced sandwich plate is investigated using HSDT kinematics (Sankar *et al.* 2014). The Mori-Tanaka method has been used to calculate material properties of the CNT reinforced sandwich plate and the linear frequency responses are investigated using refine shear deformation theory (Moradi-Dastjerdi *et al.* 2015). The FSDT kinematic relations and von Karman geometrical nonlinearity have been employed to study the post-buckling behaviour of sandwich beam reinforced with the FG-CNT (Kiani 2016). Biglari and Jafari (2010) used the FSDT kinematics to examine the natural frequency of the soft-core sandwich shell panel. The free vibration responses of the FG sandwich plate are computed by using a refined plate theory having four-variables (Hadji *et al.* 2011). The buckling and post-buckling responses of FG sandwich plate are reported (Kiani and Eslami 2012). Abdelaziz *et al.* (2017) has used different type boundary conditions to examine the mechanical responses of functionally graded sandwich plate. In addition to the above articles, many other research works have been published to illustrate the mechanical responses of the sandwich structure (Hamidi *et al.* 2015, Bennoun *et al.* 2016, Mahi *et al.* 2015, Menasria *et al.* 2017, Mehar and Panda 2017, Kolahchi *et al.* 2017b). Fundamental requirement of the composite material is obtaining the better mechanical, physical and chemical responses with lower cost and lower specific weight. In this regard, Topal and Uzman (2009) used the modified feasible direction method to optimize the frequency response of the FSDT based laminated composite structures and Kolahchi *et al.* (2017b) have implemented Grey Wolf algorithm to optimize the dynamic buckling of sandwich plate bonded with piezoelectric actuator.

From the inclusive review, it is noticed that an extensive number of research have been reported related to linear/nonlinear mechanical responses of the FG-CNT reinforced structures. However, only a few numbers of the articles are available in the open literature regarding the analysis of the nonlinear behaviour of the CNT reinforced sandwich structure. We also observe that most of the investigations are based on von-Karman type geometrical nonlinearity and the FSDT kinematics relation. So far as the authors' knowledge goes, the nonlinear deflection behaviour of the HSDT kinematics-based FG-CNT reinforced sandwich shell panel with geometrical nonlinearity in Green-Lagrange sense is yet to be published in open literature. The motive of the present research is to develop a nonlinear finite element model to examine the large deformation bending behaviour of sandwich shell panel reinforced with FG-CNT in the framework of the HSDT kinematic relations and full geometrical nonlinearity in Green-Lagrange sense. The system governing equation is derived from the variational method and the discretization is done via robust finite element steps. Finally, the nonlinear central deflection values for the sandwich shell panel with diverse grading patterns are computed by solving the final equations using a direct iterative method by means of a homemade MATLAB computer code.

2. Theory and general formulation

In this article, FG sandwich curved shell panels reinforced with CNTs are used for the nonlinear deflection analysis. The considered FG sandwich panel has length a, width b and thickness h in x, y and z-axes, respectively. The sandwich shell panels are made up of three layers, two stiff face-sheets reinforced via CNT and one isotropic layer. Stiff face-sheets are positioned at the top and bottom of the sandwich structure and the isotropic layer is positioned at the mid of both face-sheets to transfer the load between both layers, this middle layer is known as core-phase. The face-sheets are CNT reinforced via four different type CNT distribution patterns namely FG-UU (CNTs are UD in both top and bottom face-sheets), FG-ΛV (top face-sheet is graded with FG-V type and bottom face-sheet is FG-Λ type), FG-OO (both face-sheets are FG-O type CNTs distributed) and FG-XX (both face-sheets are FG-X type CNTs distributed). In which thickness of each face-sheet and core are taken as "h_f" and "h_c", respectively, as shown

Table 1 Different shell geometries

Curvature radii	Single/doubly curved shell panel				
	Plate	Spherical	Cylindrical	Hyperbolic	Elliptical
R_1	∞	R	R	R	R
R_2	∞	R	∞	-R	2R

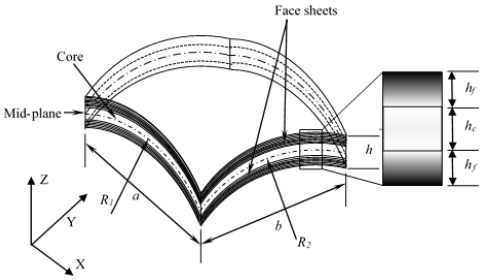

Fig. 1 FG-CNT reinforced sandwich curved shell panel

in Fig. 1. In the current analysis, four different types of geometries are used namely spherical (SPH), cylindrical (CYL), elliptical (ELL) and hyperbolic (HYP). The geometries are defined with respect to their curvature as shown in Table 1.

Both face-sheets are functionally graded and the functionally graded effective volume fraction of CNT for different grading patterns can be calculated as (Mehar and Panda 2017):

For FG-UU type distribution pattern

$$\left.\begin{aligned} V_{CNT} &= V_{CNT}^{*} \\ V_{CNT} &= 0 \end{aligned}\right\} \begin{aligned} &\text{for upper and lower face-sheets} \\ &\text{for core} \end{aligned} \tag{1}$$

For FG-ΛV type distribution pattern

$$\left.\begin{aligned} V_{CNT} &= 2\left(\frac{z_1 - z}{z_1 - z_0}\right)V_{CNT}^{*} \\ V_{CNT} &= 0 \\ V_{CNT} &= 2\left(\frac{z - z_2}{z_3 - z_2}\right)V_{CNT}^{*} \end{aligned}\right\} \begin{aligned} &\text{for lower face sheet} \\ &\text{for core} \\ &\text{for top face sheet} \end{aligned} \tag{2}$$

For FG-OO type distribution pattern

$$\left.\begin{aligned} V_{CNT} &= 2\left(1 - \left|\frac{2z - z_1 - z_0}{z_1 - z_0}\right|\right)V_{CNT}^{*} \\ V_{CNT} &= 0 \\ V_{CNT} &= 2\left(1 - \left|\frac{2z - z_3 - z_2}{z_3 - z_2}\right|\right)V_{CNT}^{*} \end{aligned}\right\} \begin{aligned} &\text{for bottom face sheet} \\ &\text{for core} \\ &\text{for top face sheet} \end{aligned} \tag{3}$$

For FG-XX type distribution pattern

$$\left.\begin{aligned} V_{CNT} &= 2\left(\left|\frac{2z - z_1 - z_0}{z_1 - z_0}\right|\right)V_{CNT}^{*} \\ V_{CNT} &= 0 \\ V_{CNT} &= 2\left(\left|\frac{2z - z_3 - z_2}{z_3 - z_2}\right|\right)V_{CNT}^{*} \end{aligned}\right\} \begin{aligned} &\text{for bottom face sheet} \\ &\text{for core} \\ &\text{for top face sheet} \end{aligned} \tag{4}$$

where, V_{CNT}^{*} is the volume fraction of CNT in each face-sheet.

2.1 Effective material properties

In the present analysis extended rule of mixture has implemented to calculate the effective material properties of the functionally graded sandwich structure.

$$E_{11} = \eta_1 V_{CNT} E_{11}^{CNT} + V_m E^m \tag{5}$$

$$\frac{\eta_2}{E_{22}} = \frac{V_{CNT}}{E_{22}^{CNT}} + \frac{V_m}{E^m} \tag{6}$$

$$\frac{\eta_3}{G_{12}} = \frac{V_{CNT}}{G_{12}^{CNT}} + \frac{V_m}{G^m} \tag{7}$$

"E_{11}, E_{22} and G_{12}" and "E_{11}^{CNT}, E_{22}^{CNT} and G_{12}^{CNT}" are represented for the longitudinal modulus of elasticity, transverse modulus of elasticity and shear modulus of the polymer composite and CNT, respectively. Similarly, E^m and G^m are the analogous notations for the polymer matrix and η_1, η_2 and η_3 are the CNT effectiveness parameters whose values are taken as same as (Shen and Xiang 2013). Superscript "*CNT*" and "*m*" represent for the CNT and matrix, respectively. In which we assumed that G_{13}=G_{12} and G_{23}=1.2G_{12} (Wang and Shen 2012b).

It is well known that the sum of the volume fraction of the fibre and matrix in the composite material is equal to one. Therefore, effective volume fractions of the matrix can be calculated as

$$V_m = 1 - V_{CNT} \tag{8}$$

Further, density (ρ), Poisson's ratio (ν_{12}) and coefficients of thermal expansion (α_{11} and α_{22}) of CNT/polymer composite are calculated as (Zhu *et al.* 2012)

$$\rho = V_{CNT}\,\rho^{CNT} + V_m \rho^m \tag{9}$$

$$\nu_{12} = V_{CNT}\nu_{11}^{CNT} + V_m \nu^m \tag{10}$$

$$\alpha_{11} = \alpha_{11}^{CNT} V_{CNT} + \alpha^m V_m \tag{11}$$

$$\alpha_{22} = (1+\upsilon_{12}^{CNT})V_{CNT}\alpha_{22}^{CNT} + (1+\upsilon^m)V_m\alpha^m - \upsilon_{12}\alpha_{11} \tag{12}$$

2.2 Kinematic model

To represent the kinematic displacement, number of shear deformation theories are proposed such as FSDT with five degree of freedom (DOF) per node (Zhu *et al.* 2012), FSDT with six DOF (Mehar and Panda 2016c), Reddy's HSDT (Reddy 2004), HSDT with nine, eleven and thirteen DOF (Natarajan *et al.* 2014), refined trigonometric shear deformation theory (Tounsi *et al.* 2013), quasi-3D sinusoidal shear deformation theory (Benchohra *et al.* 2018) refine shear deformation theory (RSDT) with five unknown variables (Hamidi *et al.* 2015), RSDT with four unknown

variables (Zidi *et al.* 2014, Bellifa *et al.* 2017, Attia *et al.* 2018, Fourn *et al.* 2018), three unknown variables hyperbolic shear deformation theory (Belabed *et al.* 2018), etc. Among all these theories, Reddy's HSDT is well known theories with good accuracy of results. In this present study, Reddy's HSDT kinematic model with nine DOF is implemented. Now, the displacement component *u*, *v* and *w* of a point along *x*, *y* and *z*-axis, respectively are explained using Taylor's series in terms of thickness coordinate as (Reddy 2004)

$$\left.\begin{aligned} u(x,y,z) &= u_0(x,y) + z u_1(x,y) + z^2 u_2(x,y) + z^3 u_3(x,y) \\ v(x,y,z) &= v_0(x,y) + z v_1(x,y) + z^2 v_2(x,y) + z^3 v_3(x,y) \\ w(x,y,z) &= w_0(x,y) \end{aligned}\right\} \tag{13}$$

where, u_0, v_0 and w_0 denote the local axial translations along the *x*, *y* and *z* directions, respectively. u_1 and v_1 represent the angular displacement of the mid-surface normal along *y* and *x*-axis, respectively. The functions u_2, u_3, v_2 and v_3 are defined as the higher order terms in the Taylor series expansion in the mid-plane of the CNT-reinforced sandwich curved shell panel. The present displacement field not only assumes parabolic shear stress variation across the panel thickness but also eliminates the use of shear correction factor (Reddy 2004). Additionally, the normal of the panel is assumed as deformable but inextensible in thickness direction. However, some researcher has considered the stretching effect to examine the mechanical responses (Draiche *et al.* 2016, Bouhadra *et al.* 2018, Younsi *et al.* 2018).

Now, the displacement field vector $\{\lambda\} = \{u \ v \ w\}^T$ can be sum up in the matrix form as

$$\{\lambda\} = [H]\{\lambda_0\} \tag{14}$$

where, the thickness coordinate matrix

$$[H] = \begin{bmatrix} 1 & 0 & 0 & z & 0 & z^2 & 0 & z^3 & 0 \\ 0 & 1 & 0 & 0 & z & 0 & z^2 & 0 & z^3 \\ 0 & 0 & 1 & 0 & 0 & 0 & 0 & 0 & 0 \end{bmatrix}$$ and

displacement field vector at mid-plane

$\{\lambda_0\}=[u_0 \ v_0 \ w_0 \ u_1 \ v_1 \ u_2 \ v_2 \ u_3 \ v_3]^T$

2.3 Strain-displacement relations

The strain-displacement relations of the FG sandwich curved shell panel using Green-Lagrange type full geometrical nonlinearity is expressed as (Reddy 2004)

$$\{\varepsilon_{ij}\} = \begin{Bmatrix} \varepsilon_{xx} \\ \varepsilon_{yy} \\ \gamma_{xy} \\ \gamma_{zx} \\ \gamma_{yz} \end{Bmatrix} = \begin{Bmatrix} \left(\frac{\partial u}{\partial x} + \frac{w}{R_x}\right) \\ \left(\frac{\partial v}{\partial y} + \frac{w}{R_y}\right) \\ \left(\frac{\partial u}{\partial y} + \frac{\partial v}{\partial x} + \frac{2w}{R_{xy}}\right) \\ \left(\frac{\partial u}{\partial z} + \frac{\partial w}{\partial x} - \frac{u}{R_x}\right) \\ \left(\frac{\partial v}{\partial z} + \frac{\partial w}{\partial y} - \frac{v}{R_y}\right) \end{Bmatrix} + \begin{Bmatrix} \frac{1}{2}\left[\left(\frac{\partial u}{\partial x} + \frac{w}{R_x}\right)^2 + \left(\frac{\partial v}{\partial x} + \frac{w}{R_{xy}}\right)^2 + \left(\frac{\partial w}{\partial x} - \frac{u}{R_x}\right)^2\right] \\ \frac{1}{2}\left[\left(\frac{\partial u}{\partial y} + \frac{w}{R_{xy}}\right)^2 + \left(\frac{\partial v}{\partial y} + \frac{w}{R_y}\right)^2 + \left(\frac{\partial w}{\partial y} - \frac{v}{R_y}\right)^2\right] \\ \left[\left(\frac{\partial u}{\partial x} + \frac{w}{R_x}\right)\left(\frac{\partial u}{\partial y} + \frac{w}{R_{xy}}\right) + \left(\frac{\partial v}{\partial x} + \frac{w}{R_{xy}}\right)\left(\frac{\partial v}{\partial y} + \frac{w}{R_y}\right) + \left(\frac{\partial w}{\partial x} - \frac{u}{R_x}\right)\left(\frac{\partial w}{\partial y} - \frac{v}{R_y}\right)\right] \\ \left[\frac{\partial u}{\partial z}\left(\frac{\partial u}{\partial x} + \frac{w}{R_x}\right) + \frac{\partial v}{\partial z}\left(\frac{\partial v}{\partial x} + \frac{w}{R_{xy}}\right) + \frac{\partial w}{\partial z}\left(\frac{\partial w}{\partial x} - \frac{u}{R_x}\right)\right] \\ \left[\frac{\partial u}{\partial z}\left(\frac{\partial u}{\partial y} + \frac{w}{R_{xy}}\right) + \frac{\partial v}{\partial z}\left(\frac{\partial v}{\partial y} + \frac{w}{R_y}\right) + \frac{\partial w}{\partial z}\left(\frac{\partial w}{\partial y} - \frac{v}{R_y}\right)\right] \end{Bmatrix} \tag{15}$$

or $\{\varepsilon_{ij}\} = \{\varepsilon_L\} + \{\varepsilon_{NL}\}$

$$\{\varepsilon_{ij}\} = \begin{Bmatrix} \varepsilon_{xx} \\ \varepsilon_{yy} \\ \gamma_{xy} \\ \gamma_{zx} \\ \gamma_{yz} \end{Bmatrix} = \begin{Bmatrix} \varepsilon_x^0 \\ \varepsilon_y^0 \\ \varepsilon_{xy}^0 \\ \varepsilon_{zx}^0 \\ \varepsilon_{yz}^0 \end{Bmatrix} + \begin{Bmatrix} \varepsilon_x^4 \\ \varepsilon_y^4 \\ \varepsilon_{xy}^4 \\ \varepsilon_{zx}^4 \\ \varepsilon_{yz}^4 \end{Bmatrix} + z\begin{Bmatrix} k_x^1 \\ k_y^1 \\ k_{xy}^1 \\ k_{zx}^1 \\ k_{yz}^1 \end{Bmatrix} + \begin{Bmatrix} k_x^5 \\ k_y^5 \\ k_{xy}^5 \\ k_{zx}^5 \\ k_{yz}^5 \end{Bmatrix} + z^2\begin{Bmatrix} k_x^2 \\ k_y^2 \\ k_{xy}^2 \\ k_{zx}^2 \\ k_{yz}^2 \end{Bmatrix} + \begin{Bmatrix} k_x^6 \\ k_y^6 \\ k_{xy}^6 \\ k_{zx}^6 \\ k_{yz}^6 \end{Bmatrix}$$
$$+ z^3\begin{Bmatrix} k_x^3 \\ k_y^3 \\ k_{xy}^3 \\ k_{zx}^3 \\ k_{yz}^3 \end{Bmatrix} + \begin{Bmatrix} k_x^7 \\ k_y^7 \\ k_{xy}^7 \\ k_{zx}^7 \\ k_{yz}^7 \end{Bmatrix} + z^4\begin{Bmatrix} k_x^8 \\ k_y^8 \\ k_{xy}^8 \\ k_{zx}^8 \\ k_{yz}^8 \end{Bmatrix} + z^5\begin{Bmatrix} k_x^9 \\ k_y^9 \\ k_{xy}^9 \\ k_{zx}^9 \\ k_{yz}^9 \end{Bmatrix} + z^6\begin{Bmatrix} k_x^{10} \\ k_y^{10} \\ k_{xy}^{10} \\ k_{zx}^{10} \\ k_{yz}^{10} \end{Bmatrix} \tag{16}$$

Further, Eq. (16) can be rearranged in the matrix form

$$\{\varepsilon\} = [H_L]\{\bar{\varepsilon}_L\} + [H_{NL}]\{\bar{\varepsilon}_{NL}\} \tag{17}$$

where, the linear and nonlinear strain vectors at mid-plane is expressed as

$\{\bar{\varepsilon}_L\} = \{\varepsilon_x^0 \ \varepsilon_y^0 \ \varepsilon_{xy}^0 \ \varepsilon_{zx}^0 \ \varepsilon_{yz}^0 \ k_x^1 \ k_y^1 \ k_{xy}^1 \ k_{zx}^1 \ k_{yz}^1 \ k_x^2 \ k_y^2 \ k_{xy}^2 \ k_{zx}^2 \ k_{yz}^2 \ k_x^3 k_y^3 \ k_{xy}^3 \ k_{zx}^3 \ k_{yz}^3\}^T$

and

$$\{\bar{\varepsilon}_{NL}\} = \begin{Bmatrix} \varepsilon_x^4 \ \varepsilon_y^4 \ \varepsilon_{xy}^4 \ \varepsilon_{zx}^4 \ \varepsilon_{yz}^4 \ k_x^5 \ k_y^5 \ k_{xy}^5 \ k_{zx}^5 \ k_{yz}^5 \ k_x^6 \ k_y^6 \ k_{xy}^6 \ k_{zx}^6 \ k_{yz}^6 \ k_x^7 k_y^7 \ k_{xy}^7 \ k_{zx}^7 \ k_{yz}^7 \\ k_x^8 k_y^8 \ k_{xy}^8 \ k_{zx}^8 \ k_{yz}^8 \ k_x^9 k_y^9 \ k_{xy}^9 \ k_{zx}^9 \ k_{yz}^9 \ k_x^{10} k_y^{10} \ k_{xy}^{10} \ k_{zx}^{10} \ k_{yz}^{10} \end{Bmatrix}^T,$$

respectively. For the detail of the individual terms can be referred (Kar and Panda 2014). Similarly, the linear thickness coordinate matrix $[H_L]$ and the nonlinear thickness coordinate matrix $[H_{NL}]$ are given as

$$[H_L] = \begin{bmatrix} 1 & 0 & 0 & 0 & 0 & z & 0 & 0 & 0 & 0 & z^2 & 0 & 0 & 0 & 0 & z^3 & 0 & 0 & 0 & 0 \\ 0 & 1 & 0 & 0 & 0 & 0 & z & 0 & 0 & 0 & 0 & z^2 & 0 & 0 & 0 & 0 & z^3 & 0 & 0 & 0 \\ 0 & 0 & 1 & 0 & 0 & 0 & 0 & z & 0 & 0 & 0 & 0 & z^2 & 0 & 0 & 0 & 0 & z^3 & 0 & 0 \\ 0 & 0 & 0 & 1 & 0 & 0 & 0 & 0 & z & 0 & 0 & 0 & 0 & z^2 & 0 & 0 & 0 & 0 & z^3 & 0 \\ 0 & 0 & 0 & 0 & 1 & 0 & 0 & 0 & 0 & z & 0 & 0 & 0 & 0 & z^2 & 0 & 0 & 0 & 0 & z^3 \end{bmatrix}$$

$$[H_{NL}] = \begin{bmatrix} 1 & 0 & 0 & 0 & 0 & z & 0 & 0 & 0 & 0 & z^2 & 0 & 0 & 0 & 0 & z^3 & 0 & 0 & 0 & 0 \\ 0 & 1 & 0 & 0 & 0 & 0 & z & 0 & 0 & 0 & 0 & z^2 & 0 & 0 & 0 & 0 & z^3 & 0 & 0 & 0 \\ 0 & 0 & 1 & 0 & 0 & 0 & 0 & z & 0 & 0 & 0 & 0 & z^2 & 0 & 0 & 0 & 0 & z^3 & 0 & 0 \\ 0 & 0 & 0 & 1 & 0 & 0 & 0 & 0 & z & 0 & 0 & 0 & 0 & z^2 & 0 & 0 & 0 & 0 & z^3 & 0 \\ 0 & 0 & 0 & 0 & 1 & 0 & 0 & 0 & 0 & z & 0 & 0 & 0 & 0 & z^2 & 0 & 0 & 0 & 0 & z^3 \\ z^4 & 0 & 0 & 0 & 0 & z^5 & 0 & 0 & 0 & 0 & z^6 & 0 & 0 & 0 & 0 & 0 & 0 & 0 & 0 & 0 \\ 0 & z^4 & 0 & 0 & 0 & 0 & z^5 & 0 & 0 & 0 & 0 & z^6 & 0 & 0 & 0 & 0 & 0 & 0 & 0 & 0 \\ 0 & 0 & z^4 & 0 & 0 & 0 & 0 & z^5 & 0 & 0 & 0 & 0 & z^6 & 0 & 0 & 0 & 0 & 0 & 0 & 0 \\ 0 & 0 & 0 & z^4 & 0 & 0 & 0 & 0 & z^5 & 0 & 0 & 0 & 0 & z^6 & 0 & 0 & 0 & 0 & 0 & 0 \\ 0 & 0 & 0 & 0 & z^4 & 0 & 0 & 0 & 0 & z^5 & 0 & 0 & 0 & 0 & z^6 & 0 & 0 & 0 & 0 & 0 \end{bmatrix}$$

2.4 Stress-strain relation

In the present analysis, three layers sandwich is used for analysis purpose. The layer-wise stress-strain relationship can be written as: (Reddy 2004)

$$\begin{Bmatrix} \sigma_{xx} \\ \sigma_{yy} \\ \tau_{xy} \end{Bmatrix}^k = \begin{bmatrix} \bar{Q}_{11} & \bar{Q}_{12} & 0 \\ \bar{Q}_{21} & \bar{Q}_{22} & 0 \\ 0 & 0 & \bar{Q}_{66} \end{bmatrix}^k \left(\begin{Bmatrix} \varepsilon_{xx} \\ \varepsilon_{yy} \\ \gamma_{xy} \end{Bmatrix} - \begin{Bmatrix} \alpha_{11} \\ \alpha_{22} \\ 0 \end{Bmatrix} \Delta T \right)^k,$$

$$\begin{Bmatrix} \tau_{zx} \\ \tau_{yz} \end{Bmatrix}^k = \begin{bmatrix} \bar{Q}_{55} & 0 \\ 0 & \bar{Q}_{44} \end{bmatrix}^k \begin{Bmatrix} \gamma_{zx} \\ \gamma_{yz} \end{Bmatrix}^k \tag{18}$$

or $\{\sigma\}^k = [Q]^k \{\varepsilon - \alpha \Delta T\}^k$

where, $\{\bar{Q}_{ij}\}$ is the stiffness matrix of the k^{th} layer of

sandwich shell panel (Wang and Shen 2012b). Subscript k = 1, 2 and 3 represented the lowest face-sheet, core and upper face-sheet, respectively. $\Delta T=T-T_0$ is change in temperature of the sandwich shell panel. T is final temperature and T_0 = 300K is the room temperature.

2.5 Finite element implementation

FEM is known to the most versatile numerical technique, mostly used to examine the mechanical behaviour of the complex geometrical structure. In the present analysis, the governing equation of the functionally graded sandwich curved shell panel is discretized using Lagrangian elements with nine nodes and each node having nine degrees of freedom associated with it. Now, using the nodal displacement vector $\{\lambda_{0i}\}$ and shape function N_i the mid-plane displacement vector $\{\lambda_0\}$ of the sandwich structure can be expressed as (Cook *et al.* 2009)

$$\{\lambda_0\}=\sum_{i=1}^{9} N_i\{\lambda_{0i}\} \tag{19}$$

where 'i' is the node number and

$\{\lambda_{0i}\}=[u_{0i}\ v_{0i}\ w_{0i}\ u_{1i}\ v_{1i}\ u_{2i}\ v_{2i}\ u_{3i}\ v_{3i}]^T$.

Using FEM, the linear mid-plane strain vector and the nonlinear mid-plane strain vector can be written in terms of nodal displacement vectors and concede as (Cook *et al.* 2009)

$$\{\bar{\varepsilon}_L\}=[B]\{\lambda_{0_i}\},\{\bar{\varepsilon}_G\}=[B_G]\{\lambda_{0_i}\}\ \{\bar{\varepsilon}_{NL}\}=[A][G]\{\lambda_{0_i}\} \tag{20}$$

where, $[B]$, $[B_G]$ and $[G]$ are the linear strain-displacement matrices associated with the shape functions and the differential operators. Similarly, $[A]$ is utilized to define the nonlinear strain and dependent on the linear displacement. The detailed regarding the individual matrices can also see from the available source (Mehar and Panda 2016b).

2.6 Work done

The functionally graded sandwich shell panel is exposed under the mechanical and thermal load. Therefore, total work done due to both types of loading can be computed as

$$W=\iint\{\lambda_0\}^T\{q\}\,dxdy+\iint\left(\{\varepsilon\}^T[Q]\{\varepsilon_{th}\}\right)dxdy \tag{21}$$

where, q is the externally mechanical load.

In the present study, two types of the external mechanical loading are included mathematically for the analysis purpose. The loading patterns are defined as the uniformly distributed load (UDL) and the sinusoidal distributed load (SDL).

I. UDL: External applied mechanical load is uniformly distributed on entire shell geometry, such that $q(x,y)=q_0$

II. SDL: The load is assumed to be distributed on the whole structure via a sinusoidal function expressed as: $q(x,y)=q_0\sin(\pi x/a)\sin(\pi y/b)$. The load value is maximum at the middle section of the panel whereas zero at all edges.

2.7 Strain energy

The FG sandwich curved shell panel under mechanical load stores strain energy expressed as

$$U=\frac{1}{2}\iint\sum_{k=1}^{3}\left[\int_{Z_{k-1}}^{Z_k}\{\varepsilon\}^T\{\sigma\}\,dz\right]dxdy \tag{22}$$

Eq. (22) can be rearranged by Eqs. (17)-(18) substitute the values of strain and stress tensors, Eq. (22) can update as

$$U=\frac{1}{2}\int_A\left(\{\bar{\varepsilon}_l\}^T[D_1]\{\bar{\varepsilon}_L\}+\{\bar{\varepsilon}_L\}^T[D_2]\{\bar{\varepsilon}_{NL}\}+\{\bar{\varepsilon}_{NL}\}^T[D_3]\{\bar{\varepsilon}_L\}+\{\bar{\varepsilon}_{NL}\}^T[D_4]\{\bar{\varepsilon}_{NL}\}\right)dA \tag{23}$$

where, $[D_1]$, $[D_2]$, $[D_3]$ and $[D_4]$ are the material property matrices, such that

$[D_1]=\sum_{k=1}^{3}\int_{Z_{k-1}}^{Z_k}[H_L]^T[\bar{Q}][H_L]dz$, $[D_2]=\sum_{k=1}^{3}\int_{Z_{k-1}}^{Z_k}[H_L]^T[\bar{Q}][H_{NL}]dz$,

$[D_3]=\sum_{k=1}^{3}\int_{Z_{k-1}}^{Z_k}[H_{NL}]^T[\bar{Q}][H_L]dz$ and $[D_4]=\sum_{k=1}^{3}\int_{Z_{k-1}}^{Z_k}[H_{NL}]^T[\bar{Q}][H_{NL}]dz$

2.8 Final governing equation

In the present analysis, the variational principle is employed to obtain the desired bending equilibrium equation of the functionally graded sandwich structure utilizing the internal energy and the external work done.

To achieve the stable equilibrium configuration of the structure, the resultant values of the energy functional should be minimum and expressed mathematically as

$$\delta\prod=\delta U-\delta W=0 \tag{24}$$

where, δ is the variational symbol and $\prod$ is the total potential energy.

Eq. (24) is rearranged further after importing the corresponding values of the energy functional and the external work done and conceded to the final form as

$$[K_s]\{\lambda_s\}=\{F_m\}+\{F_{th}\} \tag{25}$$

where, $[Ks]$ and $[\lambda s]$ are the global system stiffness matrix and global displacement vector, respectively. F_m and F_{th} are represented the global mechanical and thermal load vectors, respectively.

2.9 Solution procedure

The direct iterative method is implemented to evaluate the nonlinear deflection values of the CNT-reinforced graded sandwich panel. The detail steps of the procedural implementation can be seen in the following lines (Reddy 2004):

1. The elemental stiffness matrices and force vectors are evaluated initially following the finite element steps.
2. The global matrices and the force vectors are obtained by assembling the corresponding elemental

stiffness matrices and force vectors, respectively.

3. Compute the initial linear displacement vector from the final governing equation by dropping the appropriate nonlinear terms.

4. The nonlinear stiffness matrix is updated after the initial linear solution with the help of obtained displacement values.

5. To obtain the nonlinear displacement, repeat step 4 until the result reach the defined convergence criteria. The current convergence criterion is set as $\left(\sqrt{(\bar{W}_n - \bar{W}_{n-1})^2 / (\bar{W}_n)^2} \le \chi\right)$, where '$\bar{W}$' is central point deflection, 'n' is the number of iteration steps and 'χ =10^{-3} is the tolerance for the convergence, respectively.

3. Results and discussion

In this article, an HSDT based nonlinear finite element formulation incorporating Green-Lagrange nonlinearity is proposed and developed to investigate the large deformation bending responses of functionally graded sandwich curved shell panel reinforced with CNT. The direct iterative method has been employed to solve the nonlinear mathematical model via a domestic computer program developed in MATLAB environment. From the literatures, it is observed that thermal environment generally affects the composite structural responses significantly and the responses becomes accurate if the temperature dependent properties (Bouderba *et al.* 2013, Beldjelili *et al.* 2016, El-Haina *et al.* 2017) included in the analysis. Hence, the present research includes the properties of the reinforcement and the matrix are assumed to be temperature dependent. The core of the sandwich curved shell panel is assumed to be an isotropic homogeneous polymer and the corresponding temperature depended properties included as same as the source (Shen and Zhang 2010) E^m = (3.52 – 0.0034T) GPa, ρ^m=1150 kg/m^3 and α^m = 45(1+0.0005 ΔT) ×10^{-6}/K, where, ΔT= T – T_0, T=final temperature and T_0 = 300K. Similarly, FG-CNTRC is assumed to constitute the face-sheets of the sandwich curved shell panel and its temperature dependent material properties are taken as in (Mirzaei and Kiani 2016b). The elastic properties and the thermal expansion coefficient of the CNT can be expressed as the function of temperature (T in K) as P=P_0 (P_{-1} T^{-1}+1+ P_1 T^1+ P_2 T^2+ P_3 T^3). In which, P_0, P_{-1}, P_1, P_2 and P_3 are the coefficient of temperature and their detail values are presented in Table 2.

Table 2 Material properties of SW-CNT (Mirzaei and Kiani 2016)

Properties	P_{-1}	P_0	P_1	P_2	P_3
E_{11}^{CNT} (TPa)	0	6.39980	-4.338417×10^{-3}	7.430×10^{-6}	-4.45833×10^{-9}
E_{22}^{CNT} (TPa)	0	8.02155	-5.420375×10^{-3}	9.275×10^{-6}	-5.56250×10^{-9}
G_{12}^{CNT} (TPa)	0	1.40755	3.476208×10^{-3}	-6.965×10^{-6}	4.479167×10^{-9}
α_{11}^{CNT} (10^{-6} / K)	0	-1.12515	22.91688×10^{-3}	-28.87×10^{-6}	11.3625×10^{-9}
α_{22}^{CNT} (10^{-6} / K)	0	5.43715	-0.984625×10^{-4}	0.290×10^{-6}	0.01250×10^{-9}

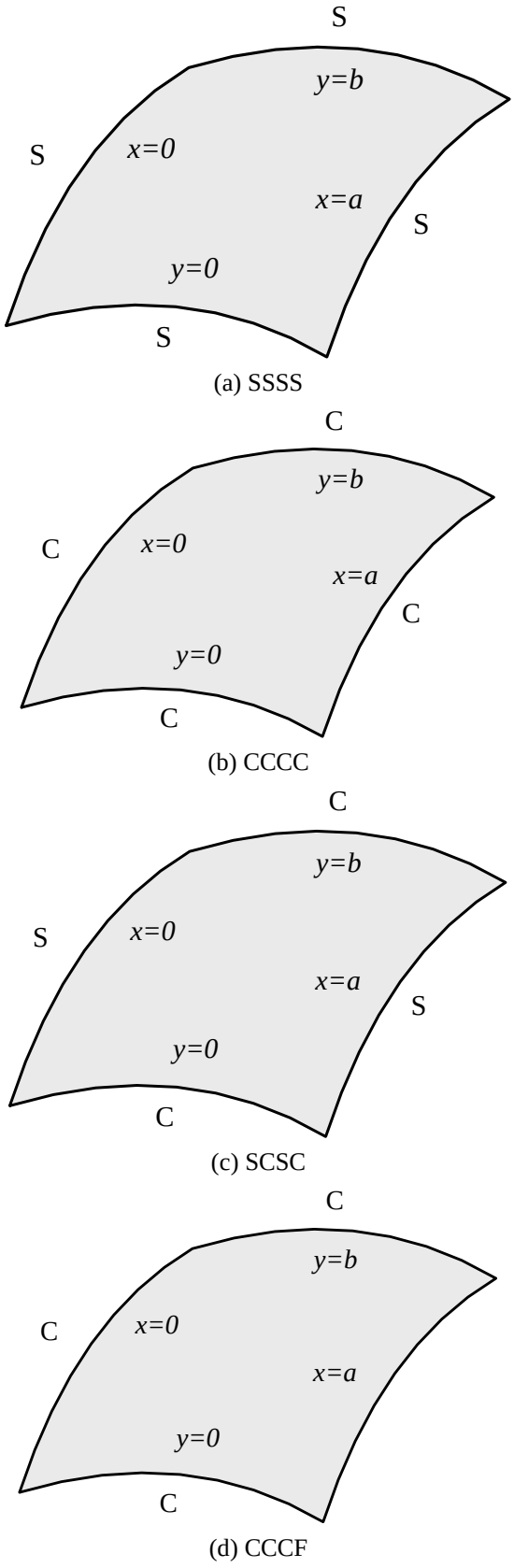

Fig. 2 Support conditions used to provide the constraint

The type of edge constraint utilized in the structural analysis affects final responses largely as it influences the final stiffness. In this regard, different research articles are

already published considering the edge effect only (Meziane *et al.* 2014, Kaci *et al.* 2018). Now, the present study also includes the various constraint conditions and their effect on the flexural strength. The different end support conditions employed in the current numerical analysis are provided in the following lines.

(a) Simply-supported boundary condition (S)

$v = w = \varphi_y = \psi_y = \theta_y = 0$ at $X = 0$, a and $u = w = \varphi_x = \psi_x = \theta_x = 0$ at $Y = 0$, b

(b) Fixed boundary condition (C)

$u = v = w = \varphi_x = \varphi_y = \psi_x = \psi_y = \theta_x = \theta_y = 0$ for both $X = 0$, a and $Y = 0$, b.

Further, the given edge support including the combination four boundaries are employed for the current analysis namely, SSSS, CCCC, SCSC and CCCF (Fig. 2).

The linear and nonlinear central deflections of the sandwich curved shell panel are normalized using the formula $\bar{W}_c = W_c / h$. where, W_c is deflection at the centre point of the plate and $\bar{W}_c$ is the normalized central deflection. The thickness of the sandwich structure is taken as 5 mm, if not stated otherwise.

3.1 Convergence and validation study

In finite element analysis, optimization of mesh size is an essential step to obtain the accurate results with minimum computational cost as both the accuracy and the computational cost increases with increasing mesh size. As a first step, the nonlinear central deflection values of cylindrical shell panels with increasing mesh size are computed for two different core to face thickness ratios (h_c/h_f=1 and 3) and four types of CNT distribution (FG-UU, FG-AV, FG-OO and FG-XX) and displayed in Fig. 3. It is observed that the responses computed using the present model are converging well with mesh refinement and a (6×6) will be stable enough for computing the desired results for throughout the analysis.

In this section, the reliability of the present nonlinear FE model has been demonstrated through diverse comparison studies. First, the nonlinear central point deflection of the laminated sandwich plate (0/90/core/90/0) is obtained via present scheme (HSDT with Green-Lagrange sense nonlinearity) and compared with the previously published result solved of FE model based on the HSDT and von-Karman nonlinearity using FEM (Madhukar and Singha 2013). The material and geometrical parameters are presented in Table 3 (Madhukar and Singha 2013) and the load parameter and central point deflection are normalized using $\bar{q} = (q_0 a^4)/(E_2 h^4)$ and $\bar{W}_c = W_c / h$, respectively. The comparison study between the present and the reference results are plotted in Fig. 4. The nonlinear flexural responses of the laminated sandwich structure computed using the presently derived higher-order model are showing well compliant with the previously published results.

Further, to improve the acceptability of the derived CNT graded sandwich model, the linear flexural responses of the FG-CNTRC plate structure computed under the mechanical UDL and compared with those available published results. The linear deflection of the FG-CNT reinforced composite

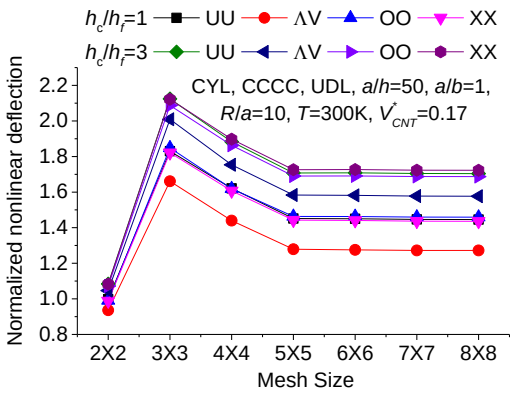

(a) Grading

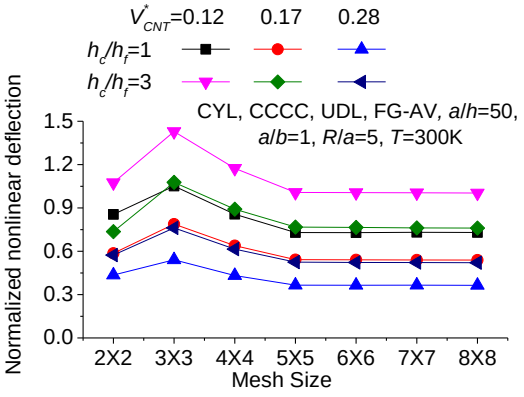

(b) CNT volume fraction

Fig. 3 Convergence study of CNT reinforced sandwich plate

Table 3 Material properties of the laminated sandwich plate

Face sheet	Core
E_1=139×10^{5}N/cm^2, E_2=9.86×10^{5}N/cm^2, G_{12}=5.24×10^{5}N/cm^2, υ_{12}= 0.3	E_c=90×10^{2}N/cm^2, G_c=32×10^{2}N/cm^2, υ_{12}=0.45

Table 4 Comparison of normalized central deflection of FG-CNTRC plate. (V^*_{CNT} =0.14, CCCC, a/b=1, q_0=0.1 MPa and 300K)

Grading configurations	a/h	FSDT (Zhu *et al.* 2012)	ANSYS (Zhu *et al.* 2012)	HSDT (Present)
UD	10	0.0021	0.0020	0.0021
	20	0.0119	0.0117	0.0119
	50	0.2131	0.2164	0.2131
FG-X	10	0.0020	0.0019	0.0020
	20	0.0104	0.0102	0.0104
	50.	0.1566	0.1584	0.1560

plate are compared with Zhu *et al.* (2012) results and presented in Table 4. Additionally, the results also computed via the simulation model developed using commercial FE package (ANSYS). In this example, the geometrical and material parameters including the end support conditions are taken as same as the source (Zhu *et al.* 2012). The close conformity between the present and the

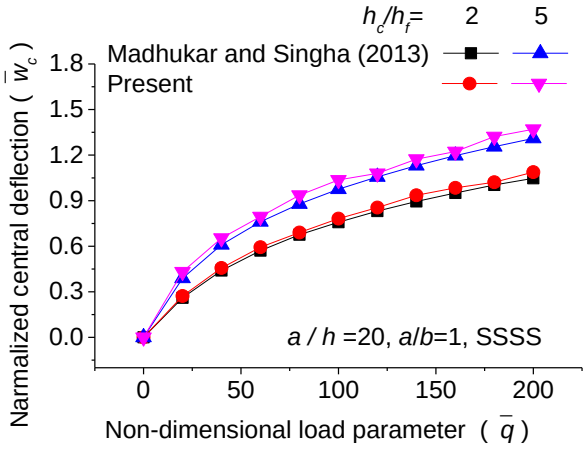

Fig. 4 Comparison of nonlinear bending behavior of laminated sandwich plate

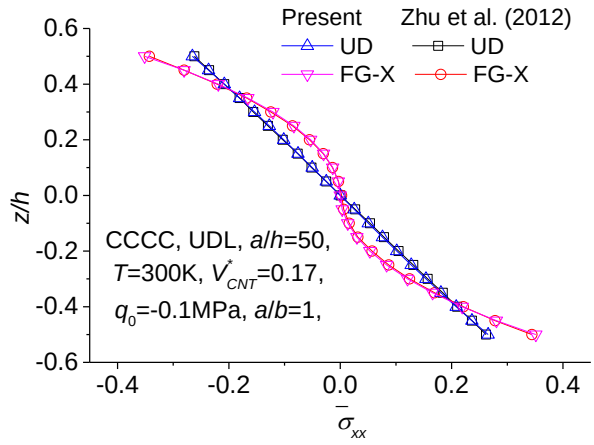

Fig. 5 Comparison of normalized in-plane stress $\bar{\sigma}_{xx} = \sigma_{xx} h^2 / \left(|q_0| a^2 \right)$ of FG-CNTRC plate

Table 5 Comparison of mid-point deflection of the functionally graded sandwich plate

Power law index (n)	Theory	$\bar{W}_c$				
		101	212	111	121	221
0	TSDT (Zenkour 2005)	0.1961	0.1961	0.1961	0.1961	0.1961
	RSDT (Bellifa *et al.* 2016)	0.1961	0.1961	0.1961	0.1961	0.1961
	Present	0.1959	0.1959	0.1959	0.1959	0.1959
1	TSDT (Zenkour 2005)	0.3236	0.3063	0.2920	0.2709	0.2809
	RSDT (Bellifa *et al.* 2016)	0.3248	0.3075	0.2930	0.2717	0.2817
	Present	0.3232	0.3059	0.2916	0.2706	0.2805
2	TSDT (Zenkour 2005)	0.3734	0.3523	0.3329	0.3026	0.3162
	RSDT (Bellifa *et al.* 2016)	0.3751	0.3541	0.3344	0.3037	0.3174
	Present	0.3729	0.3519	0.3324	0.3022	0.3158
10	TSDT (Zenkour 2005)	0.4177	0.4041	0.3855	0.3482	0.3622
	RSDT (Bellifa *et al.* 2016)	0.4192	0.4066	0.3879	0.3500	0.3640
	Present	0.4173	0.4038	0.3852	0.3478	0.3619

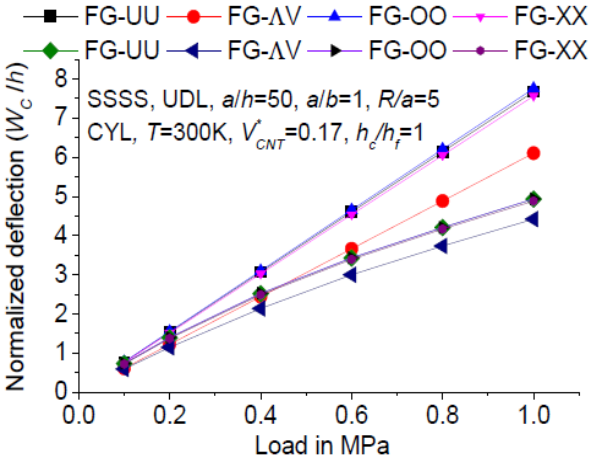

Fig. 6 Effect of CNT grading configurations on normalized central deflection of FG-CNTRC cylindrical shell panel

reference deflections clearly illustrate the validity of the currently derived higher-order model.

Another example of the simply supported functionally graded (Al/ZrO_2) square sandwich moderately thick (a/h=10) plate is solved to verify the proposed higher-order polynomial based kinematic theory. The normalized central point deflection $\bar{W}_c = 10h^3 W_c E_c / \left(a^4 |q_0| \right)$ values of the graded sandwich structural values are compared with the published data of Bellifa *et al.* (2016) and Zenkour (2005) and presented in Table 5. The present test results are showing well agreement with the source values. However, it is important to mention that the reference results are computed using the RSDT and third-order shear deformation theory (TSDT), respectively. For the computational purpose the geometrical including the material properties are taken as same as the references.

Further, the normalized in-plane stress $\left(\bar{\sigma}_{xx} = \sigma_{xx} h^2 / \left(|q_0| a^2 \right) \right)$ values are computed using the present higher-order FE model and compared with the previously published result of the reference (Zhu *et al.* 2012). For the computational purpose, two different grading configurations (UD and FG-X) are considered and the in-plane stresses are obtained at the centre point of the FG-CNTRC plate by setting the associated design parameters as: h=0.002 m, a/h=50, a/b=1, T=300K, V^*_{CNT} =0.17 and q_0=0.1 MPa with all edges clamped support condition (Zhu *et al.* 2012). The comparison between the results provided in Fig. 5 clearly indicates that the derived higher-order model also pertinent to evaluate the in-plane stresses including the flexural strength accurately.

3.2 Parametric studies

After assessing the convergence and the validity of the derived geometrically nonlinear HSDT model, the influence of various design parameters on the transverse deflection responses of the FG-CNTRC sandwich shell panel including the large deformation are investigated. The results are computed and the corresponding behavior discussed in

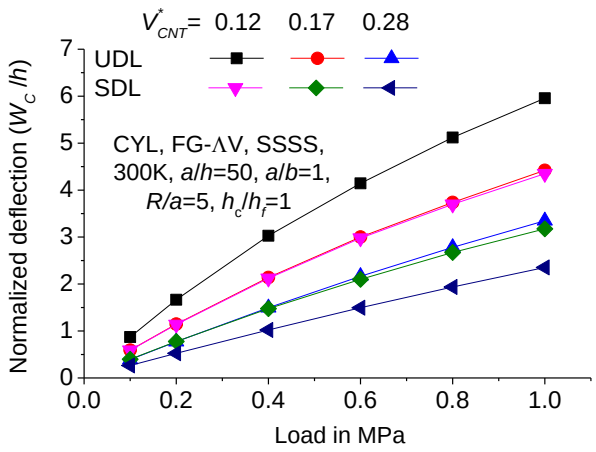

Fig. 7 Effect of CNT volume fraction on normalized central deflection of FG-CNTRC cylindrical shell panel

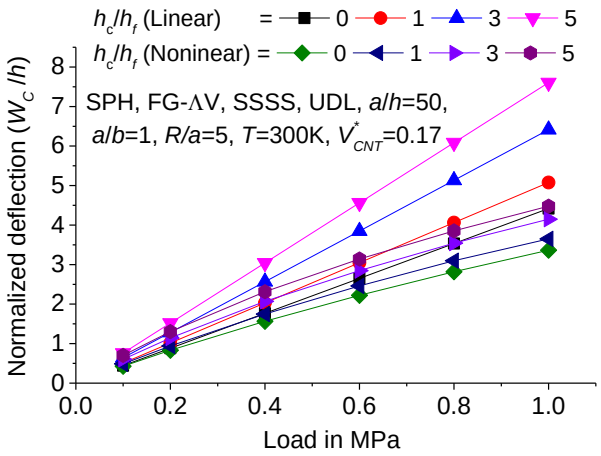

Fig. 8 Effect of core to face thickness ratio on normalized central deflection of FG-CNTRC spherical shell panel

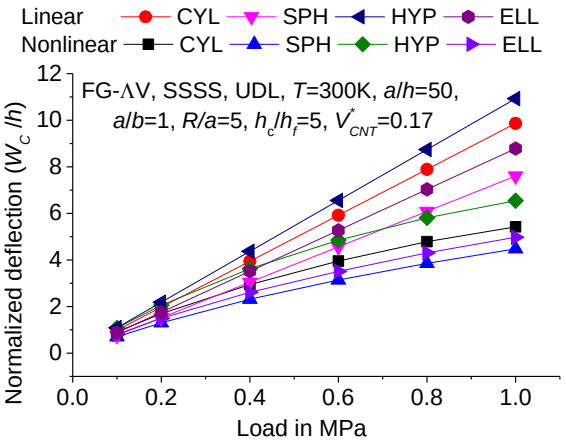

Fig. 9 Effect of geometry configuration on normalized central deflection of FG-CNTRC shell panel

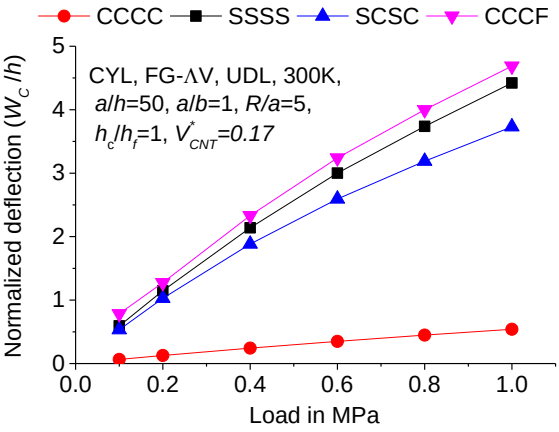

Fig. 10 Effect of support conditions on normalized central deflection of FG-CNT reinforced cylindrical sandwich panel

details.

It is expected that the type of grading configuration of the nanotube will have a significant effect on the structural responses of graded sandwich panel, since the structural stiffness varied greatly with the pattern. Therefore, the normalized central deflection values of FG-CNTRC cylindrical shell panel for four different CNT grading configurations (FG-UU, FG-ΛV, FG-OO and FG-XX) are computed in the ambient environment and shown in Fig. 6. Though both the linear and nonlinear central deflection values increase monotonously while the mechanical loading increase. However, it is worthy to note that FG-ΛV type grading indicates the stiffest configuration among all four patterns.

To study the effect of volume fractions of CNT (V^*_{CNT} = 0.12, 0.17 and 0.28) on the deflection (linear and nonlinear) parameter of CNT-reinforced FG sandwich shallow shell panel are computed for FG-ΛV type cylindrical sandwich shell panel (*a*/*b*=1, *a*/*h*=50, *R*/*a*=5, *T*=300K and h_c/h_f=1) under the influence of two different types mechanical loading (UDL and SDL) and ambient temperature. From the results as seen in Fig. 7, it can be inferred that the deflection of the FG-CNTRC sandwich shell panel decrease with higher volume fraction CNT of CNT irrespective of the types of loading. Also, the deflection values are showing higher for the UDL in comparison the SDL due to the total effective area covered in UDL higher than the SDL.

The sandwich construction strength and stiffness values are largely influenced due to the variable core to face thickness ratios, which, in turn affect the flexural responses too. The normalized linear and nonlinear central deflection values of the simply supported FG-ΛV type of sandwich spherical shell panel (*a*/*b*=1, *a*/*h*=50, *R*/*a*=5, *T*=300K and V^*_{CNT} =0.17) example has been solved for different values of core to face thickness ratio (h_c/h_f=0, 1, 3 and 5) under the mechanical UDL and ambient condition. The results are computed using the currently derived higher-order model and shown in Fig. 8. It is observed that the deflection values are increasing while the ratio (h_c/h_f) values increase. This is because of the fact that the sandwich stiffness largely depends on the face-sheet thickness. In this example, the h_c/h_f increase i.e., the sandwich core thickness increase and the structural stiffness reduced. Hence, the responses follow the expected line.

Now, to analyze the effect of geometrical configuration

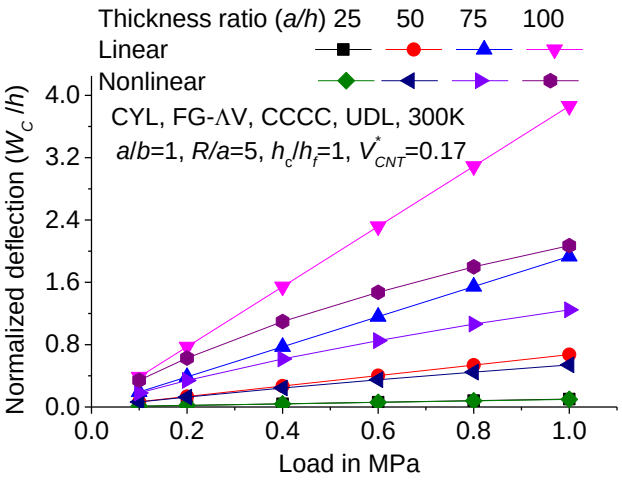

Fig. 11 Effect of thickness ratio on normalized central deflection of FG-CNT reinforced cylindrical sandwich panel

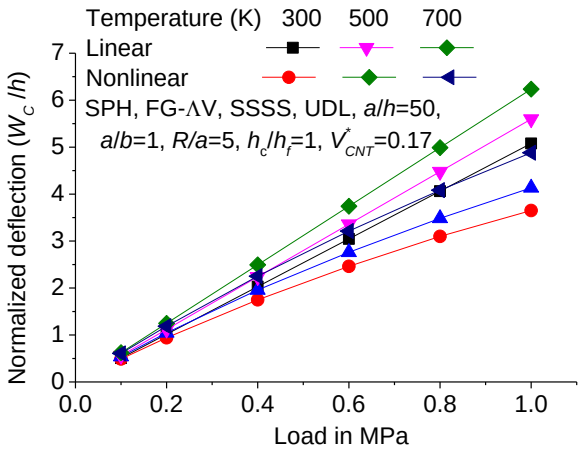

Fig. 13 Effect of temperature on normalized central deflection of FG-CNT reinforced cylindrical sandwich panel

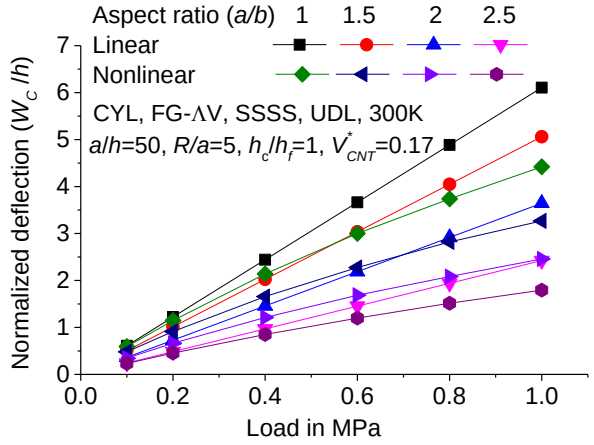

Fig. 12 Effect of aspect ratio on normalized central deflection of FG-CNT reinforced cylindrical sandwich panel

on the flexural behavior of the FG-CNTRC sandwich shell panel, the normalized central defections are computed for four different geometries (FG-ΛV, SSSS, UDL, T=300K, a/h=50, a/b=1, R/a=5, h_c/h_f=5, V^*_{CNT} =0.17) and shown in Fig. 9. The results show that the deflection is maximum for the hyperbolic (HYP) panel whereas minimum for the spherical (SPH) heometry.

Next, the influence of various edge support conditions (CCCC, CSCS, SSSS and CCCF) on the normalized central deflection of FG-CNT reinforced cylindrical sandwich panel is examined. The results are computed utilizing the associated parameters as: FG-ΛV, T=300K, a/b=1, R/a=5, V^*_{CNT} =0.17, h_c/h_f=1, UDL and shown in Fig. 10. Graphical results indicate that the normalized central deflection is minimum for all edges clamped support condition and maximum for the CCCF condition.

Fig. 11 illustrates the significance of thickness ratio (a/h=25, 50, 75 and 100) on the normalized central deflection of FG-CNT reinforced cylindrical sandwich panel (FG-ΛV, CCCC, 300K, a/b=1, R/a=5, h_c/h_f=1, V^*_{CNT} =0.17) under the UDL. The results show that the central deflection values increase for higher values of thickness ratio.

To reveal the effect of aspect ratio on the flexural responses, FG-CNT reinforced cylindrical sandwich panels (FG-ΛV, SSSS, 300K, a/h=50, R/a=5, h_c/h_f=1, V^*_{CNT} =0.17) under the UDL are considered such that the thickness (h) and thickness ratio (a/h) are constant. Therefore, width (b) decreases with increasing aspect ratio (a/b) values. Fig. 12 shows the normalized linear and nonlinear central deflections for four different aspect ratios (a/b= 1, 1.5, 2 and 2.5). It is observed that the bending responses decrease with increasing aspect ratio as for greater values of the aspect ratios the span length is decreasing in the present case.

Fig. 13 displays the linear and nonlinear central deflection of FG-ΛV type simply supported FG cylindrical sandwich shell panel (a/b=1, a/h=50, R/a =5, h_c/h_f=1 and V^*_{CNT} =0.17) subjected to UDL under the influence of three different temperature loads (T=300K, 500K and 700K). It is inferred that the linear, as well as nonlinear centre deflection of the FG cylindrical sandwich shell panel, increases with the higher value of temperature. This may be attributed to the reduction in stiffness of both the CNT and the polymer as the temperature increases.

Now, normalized in-plane stress ($\bar{\sigma}_{xx} = \sigma_{xx} h^2 / \left(|q_0| a^2\right)$) generated at the centre point (X=a/2 and Y=b/2) of the FG sandwich cylindrical shell panel is investigated for four type CNT distributions. The panel is considered to be under the UDL (q_0=0.1 MPa) with other parameters as CCCC, T=300K, a/b=1, R/a =10, a/h=50, h_c/h_f=1 and V^*_{CNT} =0.17. Fig. 14 shows the variation of in-plane stress through the thickness at the considered point of the curved panel. It is seen that the stress value is varying from bottom surface to the top surface in line with the CNT volume fraction. The stress is compressive at the top surface and tensile

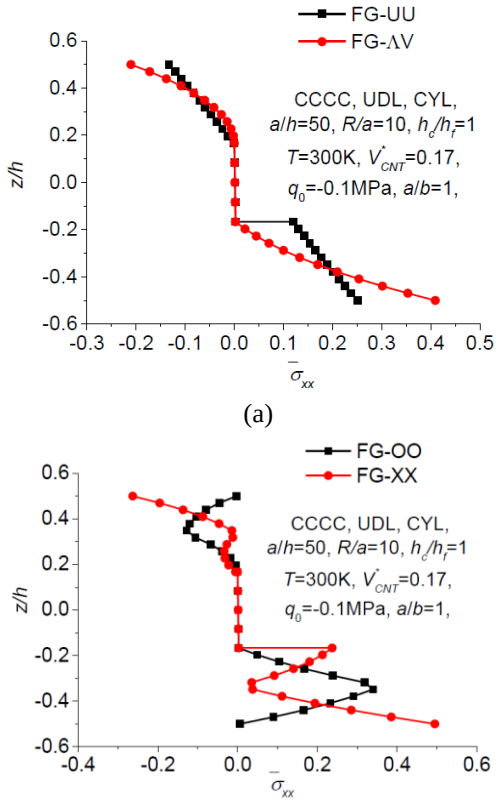

Fig. 14 Normalized in-plane stress ($\bar{\sigma}_{xx} = \sigma_{xx} h^2 / \left(|q_0| a^2 \right)$) of FG-CNT reinforced cylindrical sandwich shell panels

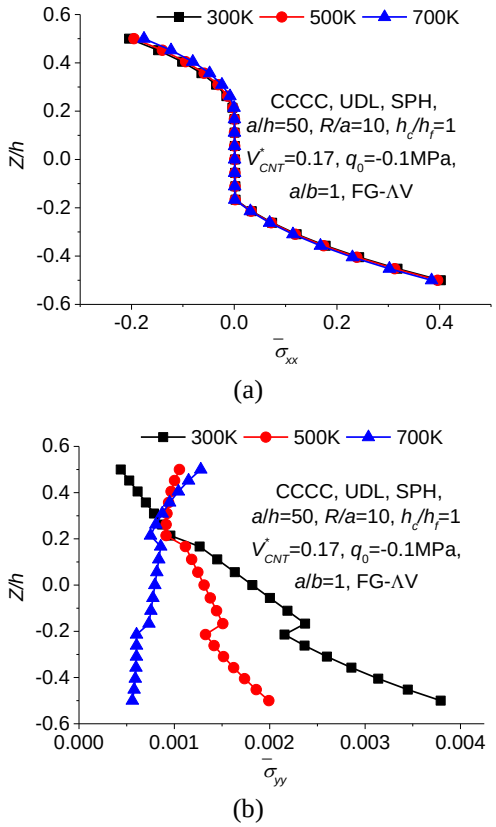

Fig. 15 Normalized in-plane stress of FG-CNT reinforced spherical sandwich panels

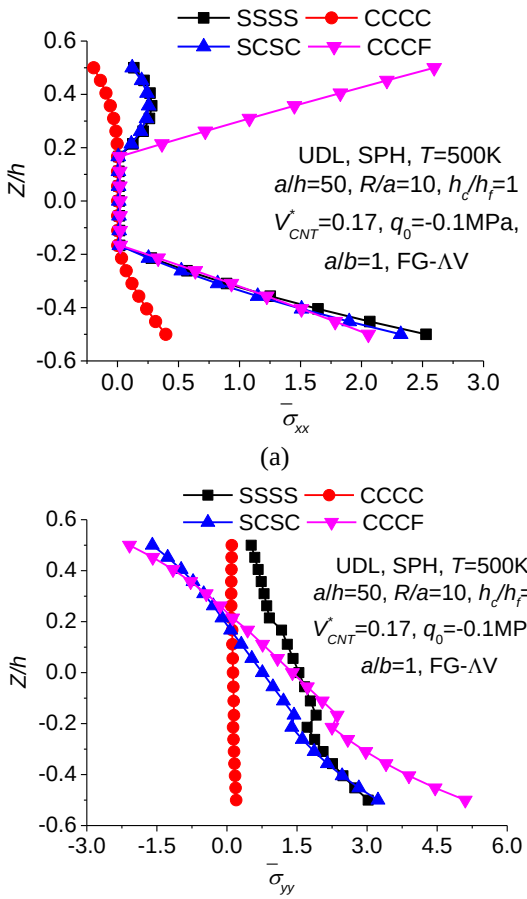

Fig. 16 Normalized in-plane stress of FG-CNT reinforced spherical sandwich panels

at the bottom surface. However, in all the cases, the stress concentration is the minimum at the core phase.

Further, the normalized stresses ($\bar{\sigma}_{xx}$ and $\bar{\sigma}_{yy}$) of the square spherical shell panel (UDL (q_0=-0.1 MPa), a/h=50, R/a=10, h_c/h_f=1, V^*_{CNT} =0.17, FG-ΛV) are computed for three different temperature loading (300K, 500K and 700K with CCCC support condition), four different support conditions (T=500K) and the results provided in figure form (Figs. 15 and 16). It is observed from Fig. 15 that the longitudinal stress (along with the x-axis) variation due to temperature change is very low whereas the stress variation in the transverse direction (y-axis) is considerable. It is because the coefficient of thermal expansion of the CNT in the transverse direction is higher than the longitudinal direction. Fig. 16 shows that the in-plane stress variation is the minimum for CCCC type support condition whereas the stress variation is the maximum for CCCF type support condition as expected.

4. Conclusions

The geometrically nonlinear flexural responses of the FG-CNT reinforced sandwich shell panel are investigated using the HSDT kinematic relation and the full nonlinearity

via Green-Lagrange strain. The governing equation is derived by the minimization of the total potential energy and solved using FEM in association with the direct iterative method. The nonlinear central deflection values are computed under the combined thermomechanical loading and the temperature dependent properties of the sandwich constituents (polymer and CNT). Further, the linear and nonlinear flexural responses are calculated for various design parameters using the novel nonlinear finite element model. The convergence and the comparison study shows that the derived nonlinear higher-order FE model for the nanotube-reinforced sandwich structure not only stable but also accurate. The normalized central deflection values increase while the temperature loading, the thickness ratios and the core to face thickness ratios increases for the curved panel whereas showing a stiffer configuration for the increasing CNT volume fractions and the aspect ratios. The normalized central deflection values are showing the minimum for the clamped type of support condition. However, the FG-ΛV type graded configuration is the stiffest configuration in comparison to other cases. The central deflection values are showing higher for the UDL in comparison to the SDL irrespective of geometry and CNT pattern.

References

Abdelaziz, H.H., Meziane, M.A.A., Bousahla, A.A., Tounsi, A., Mahmoud, S.R. and Alwabli, A.S. (2017), "An efficient hyperbolic shear deformation theory for bending, buckling and free vibration of FGM sandwich plates with various boundary conditions", *Steel Compos. Struct.*, **25**, 693-704.

Arani, A.G. and Kolahchi, R. (2014), "Nonlinear vibration and instability of embedded double-walled carbon nanocones based on nonlocal timoshenko beam theory", *J. Mech. Eng. Sci.*, **228**, 690-702.

Attia, A., Bousahla, A.A., Tounsi, A., Mahmoud, S.R. and Alwabli, A.S. (2018), "A refined four variable plate theory for thermoelastic analysis of FGM plates resting on variable elastic foundations", *Struct. Eng. Mech.*, **65**, 453-464.

Belabed, Z., Bousahla, A.A., Houari, M.S.A. Tounsi, A. and Mahmoud, S.R. (2018), "A new 3-unknown hyperbolic shear deformation theory for vibration of functionally graded sandwich plate", *Earthq. Struct.*, **14**, 103-115.

Beldjelili, Y., Tounsi, A. and Mahmoud, S.R. (2016), "Hygro-thermo-mechanical bending of S-FGM plates resting on variable elastic foundations using a four-variable trigonometric plate theory", *Smart Struct. Syst.*, **18**, 755-786.

Bellifa, H., Bakora, A., Tounsi, A., Bousahla, A.A. and Mahmoud, S.R. (2017), "An efficient and simple four variable refined plate theory for buckling analysis of functionally graded plates", *Steel Compos. Struct.*, **25**, 257-270.

Bellifa, H., Benrahou, K.H., Bousahla, A.A. Tounsi, A. and Mahmoud, S.R. (2017), "A nonlocal zeroth-order shear deformation theory for nonlinear postbuckling of nanobeams", *Struct. Eng. Mech.*, **62**, 695-702.

Bellifa, H., Halim, K., Hadji, B.L., Houari, M.S.A. and Tounsi, A. (2016), "Bending and free vibration analysis of functionally graded plates using a simple shear deformation theory and the concept the neutral surface position", *J. Brazil. Soc. Mech. Sci. Eng.*, **38**, 265-275.

Benchohra, M., Driz, H., Bakora, A., Tounsi, A., Adda Bedia, E.A. and Mahmoud, S.R. (2018), "A new quasi-3D sinusoidal shear deformation theory for functionally graded plates", *Struct. Eng. Mech.*, **65**, 19-31.

Bennoun, M., Houari, M.S.A. and Tounsi, A. (2016), "A novel five variable refined plate theory for vibration analysis of functionally graded sandwich plates", *Mech. Adv. Mater. Struct.*, **23**, 423-431.

Besseghier, A., Heireche, H., Bousahla, A.A., Tounsi, A. and Benzair, A. (2015), "Nonlinear vibration properties of a zigzag single-walled carbon nanotube embedded in a polymer matrix", *Adv. Nano Res.*, **3**, 29-37.

Biglari, H. and Jafari, A.A. (2010) "High-order free vibrations of doubly-curved sandwich panels with flexible core based on a refined three-layered theory", *Compos. Struct.*, **92**, 2685-2694.

Bilouei, B.S., Kolahchi, R. and Bidgoli, M.R. (2016), "Buckling of concrete columns retrofitted with nano-fiber reinforced Polymer (NFRP)", *Comput. Concrete*, **18**, 1053-1063.

Bouderba, B., Houari, M.S.A. and Tounsi, A. (2013), "Thermomechanical bending response of FGM thick plates resting on Winkler-Pasternak elastic foundations", *Steel Compos. Struct.*, **14**, 85-104.

Bouhadra, A., Tounsi, A., Bousahla, A.A., Benyoucef, S. and Mahmoud, S.R. (2018), "Improved HSDT accounting for effect of thickness stretching in advanced composite plates", *Struct. Eng. Mech.*, **66**(1), 61-73.

Chen, X.L. and Liu, Y.J. (2004), "Square representative volume elements for evaluating the effective material properties of carbon nanotube-based composites", *Comput. Mater. Sci.*, **29**, 1-11.

Cividanes, L.S., Simonetti, E.A.N., Moraes, M.B., Fernandes, F.W. and Thim, G.P. (2014), "Influence of carbon nanotubes on epoxy resin cure reaction using different techniques: A comprehensive review", *Polym. Eng. Sci.*, **54**, 2461-2469.

Cook, R.D., Malkus, D.S., Plesha, M.E. and Witt, R.J. (2009), *Concepts and Applications of Finite Element Analysis*, 4th Edition, John Wiley & Sons Pvt. Ltd., Singapore.

Draiche, K., Tounsi, A. and Mahmoud, S.R. (2016), "A refined theory with stretching effect for the flexure analysis of laminated composite plates", *Geomech. Eng.*, **11**, 671-690.

El-Haina, F., Bakora, A., Bousahla, A.A., Tounsi, A. and Mahmoud, S.R. (2017), "A simple analytical approach for thermal buckling of thick functionally graded sandwich plates", *Struct. Eng. Mech.*, **63**, 585-595.

Esteva, M. and Spansos, P.D. (2009), "Effective elastic properties of nanotube reinforced composites with slightly weakened interfaces", *J. Mech. Mater. Struct.*, **4**, 887-900.

Fourn, H., Atmane, H.A., Bourada, M., Bousahla, A.A., Tounsi, A. and Mahmoud, S.R. (2018), "A novel four variable refined plate theory for wave propagation in functionally graded material plates", *Steel Compos. Struct.*, **27**, 109-122.

Hadji, L., Atmane, H.A., Tounsi, A., Mechab, I. and Adda Bedia, E.A. (2011), "Free vibration of functionally graded sandwich plates using four-variable refined plate theory", *Appl. Math. Mech.*, **32**, 925-942.

Hamidi, A., Houari, M.S.A., Mahmoud, S.R.R. and Tounsi, A. (2015), "A sinusoidal plate theory with 5-unknowns and stretching effect for thermomechanical bending of functionally graded sandwich plates", *Steel Compos. Struct.*, **18**, 235-253.

Henderson, J.P., Plummer, A. and Johnston, N. (2018), "An electro-hydrostatic actuator for hybrid active-passive vibration isolation", *Int. J. Hydromechatron.*, **1**, 47-71.

Heydari, M.M., Hafizi Bidgoli, A., Golshani, H.R., Beygipoor, G. and Davoodi, A. (2015), "Nonlinear bending analysis of functionally graded CNT-reinforced composite mindlin polymeric temperature-dependent plate resting on orthotropic elastomeric medium using GDQM", *Nonlin. Dyn.*, **79**, 1425-1441.

Iijima, S. (1991), "Helical microtubules of graphitic carbon", *Nat.*,

354, 56-58.
Kaci, A., Houari, M.S.A., Bousahla, A.A., Tounsi, A. and Mahmoud, S.R. (2018), "Post-buckling analysis of shear-deformable composite beams using a novel simple two-unknown beam theory", *Struct. Eng. Mech.*, **65**, 621-631.
Kaci, A., Tounsi, A., Bakhti, K. and Adda Bedia, E.A. (2012), "Nonlinear cylindrical bending of functionally graded carbon nanotube-reinforced composite plates", *Steel Compos. Struct.*, **12**, 491-504.
Kar, V.R. and Panda, S.K. (2014), "Nonlinear free vibration of functionally graded doubly curved shear deformable panels using finite element method", *J. Vibr. Contr.*, **22**, 1935-1949.
Karami, B., Janghorban, M. and Tounsi, A. (2018a), "Nonlocal strain gradient 3D elasticity theory for anisotropic spherical nanoparticles", *Steel Compos. Struct.*, **27**(2), 201-216.
Karami, B., Janghorban, M. and Tounsi, A. (2018a), "Variational approach for wave dispersion in anisotropic doubly-curved nanoshells based on a new nonlocal strain gradient higher order shell theory", *Thin-Wall. Struct.*, **129**, 251-264.
Khetir, H., Bouiadjra, M.B., Houari, M.S.A., Tounsi, A. and Mahmoud, S.R. "A new nonlocal trigonometric shear deformation theory for thermal buckling analysis of embedded nanosize FG plates", *Struct. Eng. Mech.*, **64**, 391-402.
Kiani, Y. (2016), "Thermal postbuckling of temperature-dependent sandwich beams with carbon nanotube-reinforced face sheets", *J. Therm. Stress.*, **39**, 1098-1110.
Kiani, Y. and Eslami, M.R. (2012), "Thermal buckling and post-buckling response of imperfect temperature-dependent sandwich fgm plates resting on elastic foundation", *Arch. Appl. Mech.*, **82**, 891-905.
Kolahchi, R., Keshtegar, B. and Fakhar, M.H. (2017a), "Optimization of dynamic buckling for sandwich nanocomposite plates with sensor and actuator layer based on sinusoidal-visco-piezoelasticity theories using Grey Wolf algorithm", *J. Sandw. Struct. Mater.*, DOI: 10.1177/1099636217731071.
Kolahchi, R., Safari, M. and Esmailpour, M. (2014), "Dynamic stability analysis of temperature-dependent functionally graded CNT-reinforced visco-plates resting on orthotropic elastomeric medium", *Compos. Struct.*, **150**, 255-265.
Kolahchi, R., Zarei, M.S., Hajmohammad, M.H. and Nouri, A. (2017b), "Wave propagation of embedded viscoelastic FG-CNT-reinforced sandwich plates integrated with sensor and actuator based on refined zigzag theory", *Int. J. Mech. Sci.*, **130**, 534-545.
Lei, Z.X., Liew, K.M. and Yu, J.L. (2013), "Large deflection analysis of functionally graded carbon nanotube-reinforced composite plates by the element-free kp-ritz method", *Comput. Meth. Appl. Mech. Eng.*, **256**, 189-199.
Lei, Z.X., Zhang, L.W., Liew, K.M. and Yu, J.L. (2014), "Dynamic stability analysis of carbon nanotube-reinforced functionally graded cylindrical panels using the element-free kp-ritz method", *Compos. Struct.*, **113**, 328-338.
Li, C. and Chou, T.W. (2004), "Elastic properties of single-walled carbon nanotubes in transverse directions", *Phys. Rev. B*, **69**, 2003-2005.
Madani, H., Hosseini, H. and Shokravi, M. (2016), "Differential cubature method for vibration analysis of embedded FG-CNT-reinforced piezoelectric cylindrical shells subjected to uniform and non-uniform temperature distributions", *Steel Compos. Struct.*, **22**, 889-913.
Madhukar, S. and Singha, M.K. (2013), "Geometrically nonlinear finite element analysis of sandwich plates using normal deformation theory", *Compos. Struct.*, **97**, 84-90.
Mahi, A., Bedia, E.A.A. and Tounsi, A. (2015), "A new hyperbolic shear deformation theory for bending and free vibration analysis of isotropic, functionally graded, sandwich and laminated composite plates", *Appl. Math. Modell.*, **39**, 2489-2508.
Mehar, K. and Panda, S.K. (2016a), "Geometrical nonlinear free vibration analysis of FG-CNT reinforced composite flat panel under uniform thermal field", *Compos. Struct.*, **143**, 336-346.
Mehar, K. and Panda, S.K. (2016b), "Nonlinear static behavior of FG-CNT reinforced composite flat panel under thermomechanical load", *J. Aerosp. Eng.*, **30**, 1-12.
Mehar, K. and Panda, S.K. (2016c), "Free vibration and bending behaviour of CNT reinforced composite plate using different shear deformation theory", *Mater. Sci. Eng.*, **115**, 012014.
Mehar, K. and Panda, S.K. (2017), "Thermal free vibration behavior of FG-CNT reinforced sandwich curved panel using finite element method", *Polym. Compos.*, DOI: 10.1002/pc.24266.
Menasria, A., Bouhadra, A., Tounsi, A., Bousahla, A.A. and Mahmoud, S.R. (2017), "A new and simple HSDT for thermal stability analysis of FG sandwich plates", *Steel Compos. Struct.*, **25**(2), 157-175.
Meziane, M.A.A., Abdelaziz, H.H. and Tounsi, A. (2014), "An efficient and simple refined theory for buckling and free vibration of exponentially graded sandwich plates under various boundary conditions", *J. Sandw. Struct. Mater.*, **16**, 293-318.
Mirzaei, M. and Kiani, Y. (2016), "Thermal buckling of temperature dependent FG-CNT reinforced composite plates", *Meccan.*, **51**, 2185-2201.
Moradi-Dastjerdi, R., Payganeh, G., Malek-Mohammadi, H., Dastjerdi, R.M., Payganeh, G. and Mohammadi, H.M. (2015), "Free vibration analyses of functionally graded CNT reinforced nanocomposite sandwich plates resting on elastic foundation", *J. Sol. Mech.*, **7**, 158-172.
Natarajan, S., Haboussi, M. and Manickam, G. (2014), "Application of higher-order structural theory to bending and free vibration analysis of sandwich plates with CNT reinforced composite face sheets", *Compos. Struct.*, **113**, 197-207.
Reddy, J.N. (2004), *Mechanics of Laminated Composite Plates and Shells: Theory and Analysis*, 2nd Edition, CRC Press, Boca Raton, London, New York, Washington, D.C.
Sankar, A., Natarajan, S., Haboussi, M., Ramajeyathilagam, K. and Ganapathi, M. (2014), "Panel flutter characteristics of sandwich plates with CNT reinforced facesheets using an accurate higher-order theory", *J. Flu. Struct.*, **50**, 376-391.
Shen, H.S. (2009), "Nonlinear bending of functionally graded carbon nanotube-reinforced composite plates in thermal environments", *Compos. Struct.*, **91**, 9-19.
Shen, H.S. and Xiang, Y. (2013), "Nonlinear analysis of nanotube-reinforced composite beams resting on elastic foundations in thermal environments", *Eng. Struct.*, **56**, 698-708.
Shen, H.S. and Xiang, Y. (2014), "Nonlinear vibration of nanotube-reinforced composite cylindrical panels resting on elastic foundations in thermal environments", *Compos. Struct.*, **111**, 291.
Shen, H.S. and Zhang, C.L. (2010), "Thermal buckling and postbuckling behavior of functionally graded carbon nanotube-reinforced composite plates", *Mater. Des.*, **31**, 3403-3411.
Shi, D.L., Feng, X.Q., Huang, Y.Y., Hwang, K.C. and Gao, H. (2004), "The effect of nanotube waviness and agglomeration on the elastic property of carbon nanotube-reinforced composites", *J. Eng. Mater. Technol.*, **126**, 250-257.
Szekrenyes, A. (2014), "Stress and fracture analysis in delaminated orthotropic composite plates using third-order shear deformation theory", *Appl. Math. Modell.*, **38**, 3897-3916.
Topal, U. and Uzman, U. (2009), "Frequency optimization of laminated folded composite plates", *Mater. Des.*, **30**, 494-501.
Tornabene, F., Fantuzzi, N., Bacciocchi, M. and Viola, E. (2016), "Effect of agglomeration on the natural frequencies of functionally graded carbon nanotube-reinforced laminated composite doubly-curved shells", *Compos. Part B: Eng.*, **89**,

187-218.
Tounsi, A., Houari, M.S.A., Benyoucef, S. and Adda Bedia, E.A. (2013), "A refined trigonometric shear deformation theory for thermoelastic bending of functionally graded sandwich plates", *Aerosp. Sci. Technol.*, **24**, 209-220.
Wang, Z., Xie, Z. and Huang, W. (2018), "A pin-moment model of flexoelectric actuators", *Int. J. Hydromechatron.*, **1**, 72-90.
Wang, Z.X. and Shen, H.S. (2012), "Nonlinear dynamic response of nanotube-reinforced composite plates resting on elastic foundations in thermal environments", *Nonlin. Dyn.*, **70**, 735-754.
Wang, Z.X. and Shen, H.S. (2012), "Nonlinear vibration and bending of sandwich plates with nanotube-reinforced composite face sheets", *Compos. Part B: Eng.*, **43**, 411-421.
Yas, M.H. and Heshmati, M. (2012), "Dynamic analysis of functionally graded nanocomposite beams reinforced by randomly oriented carbon nanotube under the action of moving load", *Appl. Math. Modell.*, **36**, 1371-1394.
Yazid, M., Heireche, H., Tounsi, A. Bousahla, A.A. and Houari, M.S.A. (2018), "A novel nonlocal refined plate theory for stability responsze of orthotropic single-layer graphene sheet resting on elastic medium", *Smart Struct. Syst.*, **21**, 15-25.
Youcef, D.O., Kaci, A., Benzair, A., Bousahla, A.A. and Tounsi, A. (2018), "Dynamic analysis of nanoscale beams including surface stress effects", *Smart Struct. Syst.*, **21**, 65-74.
Younsi, A., Tounsi, A., Zaoui, F.Z., Bousahla, A.A. and Mahmoud, S.R. (2018), "Novel quasi-3D and 2D shear deformation theories for bending and free vibration analysis of FGM plates", *Geomech. Eng.*, **14**, 519-532.
Zemri, A., Houari, M.S.A., Bousahla, A.A. and Tounsi, A. (2015), "A mechanical response of functionally graded nanoscale beam: an assessment of a refined nonlocal shear deformation theory beam theory", *Struct. Eng. Mech.*, **54**, 693-710.
Zenkour, A.M. (2005), "A comprehensive analysis of functionally graded sandwich plates: Part 1-deflection and stresses", *Int. J. Sol. Struct.*, **42**, 5224-5242.
Zhang, C.L. and Shen, H.S. (2006), "Temperature-dependent elastic properties of single-walled carbon nanotubes: Prediction from molecular dynamics simulation", *Appl. Phys. Lett.*, **89**, 081904.
Zhang, L.W. (2017), "Geometrically nonlinear large deformation analysis of triangular CNT-reinforced composite plates with internal columnsupports", *J. Model. Mech. Mater.*, **1**, 20160154.
Zhang, L.W., Lei, Z.X., Liew, K.M. and Yu, J.L. (2014), "Large deflection geometrically nonlinear analysis of carbon nanotube-reinforced functionally graded cylindrical panels", *Comput. Meth. Appl. Mech. Eng.*, **273**, 1-18.
Zhang, Y.Y., Wang, C.M., Tan, V.B.C., Zhang, Y.Y., Wang, C.M. and Tan, V.B.C. (2008), "Examining the effects of wall numbers on buckling behavior and mechanical properties of multiwalled carbon nanotubes via molecular dynamics simulations examining the effects of wall numbers on buckling behavior and mechanical properties of multiwalled car", *J. Appl. Phys.* **103**(5), 053505.
Zhu, P., Lei, Z.X. and Liew, K.M. (2012), "Static and free vibration analyses of carbon nanotube-reinforced composite plates using finite element method with first order shear deformation plate theory", *Compos. Struct.*, **94**, 1450-1460.
Zidi, M., Tounsi, A., Houari, M.S.A., Adda Bedia, E.A. and Anwar Bag, O. (2014), "Bending analysis of FGM plates under hygro-thermo-mechanical loading using a four variable refined plate theory", *Aerosp. Sci. Technol.*, **34**, 24-34.
Zine, A., Tounsi, A., Draiche, K., Sekkal, M. and Mahmoud, S.R. (2018), "A novel higher-order shear deformation theory for bending and free vibration analysis of isotropic and multilayered plates and shells", *Steel Compos. Struct.*, **26**, 125-137.

CC